Design and Experimental Evaluation of an Active Underwater Inflatable Co-prime Sonar Array (UICSA)

George Sklivanitis,[1†] Yanjun Li,[2] Konstantinos Tountas,[1] Bing Ouyang,[2] Jordan Thomas,[2]
Tsung-Chow Su,[3] and Dimitris Pados[1]

[1]I-SENSE and Dept. of Comp. and Electrical Eng. & Computer Sc., Florida Atlantic University, Boca Raton, FL
E-mail: {gsklivanitis, ktountas2017, dpados}@fau.edu
[2]Harbor Branch Oceanographic Institute, Florida Atlantic University, Ft. Pierce, FL
E-mail: {yli2013, bouyang}@fau.edu, jbt18@vt.edu
[3]Dept. of Ocean and Mechanical Engineering, Florida Atlantic University, Boca Raton, FL
E-mail: su@fau.edu

***Abstract*—We consider underwater target detection by using a novel active, self-contained and rapidly deployable underwater inflatable co-prime sonar array (UICSA). In particular, we measure the received signal strength (RSS) and angle-of-arrival (AoA) of acoustic signals reflected by an underwater target. Measurements from different positions of the transmitter with respect to the UICSA are organized in a three mode real-valued tensor. Then, the conformity of each entry with respect to all other data points in the tensor is calculated based on recursively refined calculations of L_1-norm tensor subspaces. Conformity values are then used for the detection of an underwater target. We evaluate the data conformity of RSS and AoA recordings acquired from the testbed deployment of a seven-element UICSA prototype and three underwater acoustic transmitters at Florida Atlantic University. We show for the first time that conformity evaluation over multi-modal data measurements can accurately detect the presence of an underwater target.**

I. Introduction

Underwater-acoustic (UW-A) sensor networks have attracted considerable attention for both military and commercial applications including marine life monitoring, offshore oil exploration, underwater navigation and surveillance, and sonar detection [1]–[4]. Target tracking is one of the important applications of underwater wireless sensor networks. Autonomous underwater vehicles (AUVs) can be used to detect underwater targets that cannot be detected by fixed sensor nodes. AUVs are a practical device for monitoring, observing and inspecting the ocean.

Sonar systems have the capability to estimate both spatial and temporal wave fronts however, the most essential mission of sonar arrays is the estimation of direction-of-arrival (DOA), i.e., bearing information. Active sonar systems provide both range and bearing information. Three different types of active sonar systems are used to detect and track the target: mono-static (both transmitter and receiver are co-located), bistatic (receiver is separated from transmitter), and multi-static (one transmitter and multiple receivers). Passive sonar systems are used to analyze the features of AUVs. Due to the advantages of target tracking based on three-dimensional (3D) measurements and sensor management, active sonar systems have received great attention over passive sonars [5]. Fusing the information from multiple arrays typically improves the performance of target detection, tracking and ranging, even if the arrays are highly displaced and the received acoustic signals are not significantly correlated [6].

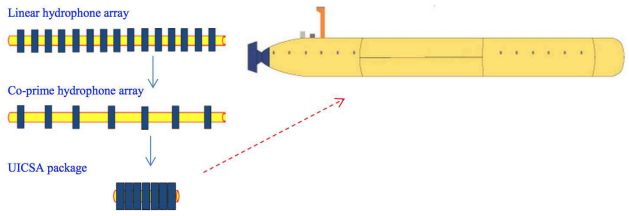

Fig. 1: The Underwater Inflatable Co-prime Sonar Array (UICSA) concept.

In this work, we consider underwater target detection using a novel active, self-contained and rapidly deployable sensor array design, namely the Underwater Inflatable Co-prime Sonar Array (UICSA). UICSA is a compact array assembly (as depicted in Fig. 1) which can be rapidly deployed in the ocean and then morph into pre-determined length to work as an active sonar array. We evaluate the UICSA design from launching to morphing as well as its operational capability as an active co-prime hydrophone array to detect the presence of an underwater target. More specifically, we use UICSA to measure the received signal strength (RSS) and angle-of-arrival (AoA) of acoustic signal transmissions in a 9 m deep acoustic water test tank at Florida Atlantic University. RSS and AoA measurements from different locations of the transmitter with respect to the position of the UICSA are organized in a

This work was supported by the National Science Foundation under Grant CNS-1753406. The work of D. A. Pados was also supported by the Schmidt Family Foundation.

[†]Principal author: George Sklivanitis, Research Assistant Professor, Department of Computer and Electrical Engineering & Computer Science, Florida Atlantic University, Boca Raton FL 33431, USA.

978-0-578-57618-3 ©2019 MTS

three mode real-valued tensor. The conformity of each tensor data point with respect to all other collected data is calculated based on recursively refined L_1-norm tensor subspaces. The developed tensor data-conformity evaluation scheme processes any given data set represented by a high-dimensional tensor and converts each data entry to a continuous zero-to-one "alert value" (zero implying highly conforming data -one implying highly non-conforming data). Detection of non-conforming data entries enhances our ability to rapidly identify materials/objects underwater. Experimental studies demonstrate the effectiveness of the tensor conformity evaluation algorithm for underwater detection of an acoustic dampening object.

II. System Model

We consider a co-prime array consisting of two uniform linear arrays (ULAs). Fig. 2 depicts a co-prime pair of uniform linear sub-arrays. The first ULA uses M hydrophone elements with an inter-element spacing of N units. The second ULA uses N elements with an inter-element spacing of M units. M and N are co-prime integers (with $M < N$) and the unit inter-element spacing, d, is usually set as half wavelength or $\lambda/2$. Because the two sub-arrays share the first sensor at the first position, the total number of hydrophone elements in the co-prime array is $M + N - 1$.

We assume acoustic transmissions of a chirp signal with duration T, and spanning frequencies from $f_{\min}$ to $f_{\max}$ that are defined as

$$s(t) = \cos\left(2\pi \frac{f_{\max} - f_{\min}}{2T} t^2 + f_{\min} t\right). \quad (1)$$

We consider transmissions from different locations than . The co-prime array collects RSS and AoA measurements, that include signal reflections off targets in the surrounding area. Then, the data vector received at the co-prime array is expressed as

$$\mathbf{x}(t) = \mathbf{a}(\phi, \theta) s(t) + \mathbf{n}(t) \quad (2)$$

where $\mathbf{n}(t)$ is additive noise and $\mathbf{a}(\phi, \theta) \in \mathbb{C}^{M+N-1}$ is the hydrophone array response vector defined as

$$\mathbf{a}(\phi, \theta) = \exp\left\{ j2\pi \frac{1}{\lambda} \mathbf{P}^T \mathbf{k}(\phi, \theta) \right\} \in \mathbb{C}^{M+N-1 \times 1} \quad (3)$$

where λ is the carrier wavelength. Matrix $\mathbf{P}$ contains the positions of the hydrophone array elements, where the first hydrophone is assumed as the reference and is written as

$$\mathbf{P} = \begin{bmatrix} x_1 & x_2 & \dots & x_{M+N-1} \\ y_1 & y_2 & \dots & y_{M+N-1} \\ z_1 & z_2 & \dots & z_{M+N-1} \end{bmatrix} \in \mathbb{R}^{3 \times M+N-1} \quad (4)$$

while the vector $\mathbf{k}(\phi, \theta)$ represents the projection of the received signal's steering vector on the hydrophone array coordinate system defined as

$$\mathbf{k}(\phi, \theta) = \begin{bmatrix} \cos(\theta)\sin(\phi) \\ \cos(\theta)\cos(\phi) \\ \sin(\theta) \end{bmatrix} \in \mathbb{R}^{3 \times 1}. \quad (5)$$

The co-prime array data are then processed using MUltiple SIgnal Classification (MUSIC)-type subspace techniques [7], [8] for the estimation of the azimuth and elevation AoAs (ϕ, θ) of the transmitted chirp signal. The number of acoustic sources that can be resolved by the co-prime array is the product of the number of elements of the two sub-arrays.

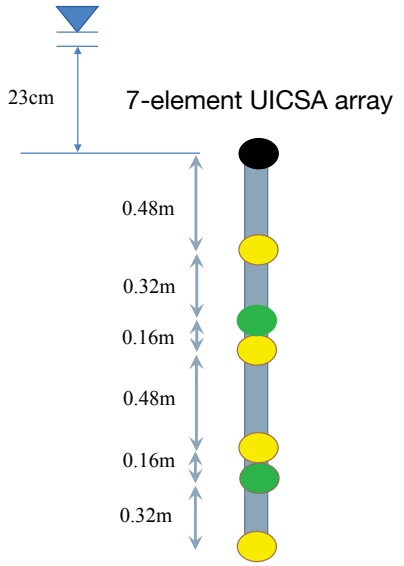

Fig. 2: UICSA array prototype dimensions comprising of two ULAs with $M = 3$ and $N = 5$ hydrophone elements.

In parallel with AoA estimation, we calculate the RSS of the transmitted chirp signal at the co-prime array. In particular, we first cross-correlate the received signal at each hydrophone element with $s(t)$. Then, at the i-th array element, the output of the matched filter is written as

$$R_i(\tau) = \frac{\int_0^{+\infty} s(t) x_i(t+\tau) \mathrm{d}t}{\left(\int_0^T x_i^2(t) \mathrm{d}t \int_0^T s(t) \mathrm{d}t \right)^{1/2}}. \quad (6)$$

We then search for cross-correlation peaks in $R_i(\tau)$ using a sliding window of length T. We select the highest peak and calculate the received signal strength at the i-th hydrophone element as

$$\mathrm{RSS}_i = \int_0^T R_i(t) \mathrm{d}t, \quad i = 1, \dots, M+N-1. \quad (7)$$

We propose to collect RSS and AoA values over time and organize these features in a real-valued matrix $\mathbf{D} \in \mathbb{R}^{(M+N+1) \times P}$, with P denoting the number of transmissions. For acoustic transmissions from K different locations in the surrounding area of the co-prime array, we propose to organize RSS and AoA data in a three mode tensor $\mathcal{D} \in \mathbb{R}^{(M+N+1) \times P \times K}$.

III. Underwater Target Detection Algorithm

The goal of the proposed underwater target detection algorithm is to leverage RSS and AoA of acoustic signal transmissions to capture reflections by underwater objects/targets by the UICSA. RSS and AoA measurements are complementary to each other for different objects. For example, when the line-of-sight (LoS) component is strong, RSS data can be useful, while if the LoS signal is blocked, RSS will be significantly weakened. However the estimated AoA values will help to strengthen the detection of an underwater object. After organizing RSS and AoA in a three mode tensor we implement a

data analysis method that directly converts the original tensor data set to a new tensor of the exact same dimensions, where each new tensor entry measures the conformity of that entry with respect to all other data points. The conformity metric will take values from the $[0, 1]$ set of real numbers, with conformity values close to 1 indicating "misbehaving" data points, and values close to 0 corresponding to nominal data points. This is achieved, by utilizing iteratively refined L_1-norm (absolute-error) data subspaces [9]–[11]. Detection of non-conforming data entries enables accurate detection of underwater objects with an active UICSA.

Given the three mode tensor $\mathcal{D} \in \mathbb{R}^{(M+N+1)\times P\times K}$, where the rows are RSS and AoA values, the columns of the tensor correspond to time, and the third dimension corresponds to different transmitter locations with respect to the array. L_1-norm principal component analysis (PCA), is by itself a fundamental data feature learning approach that is arguably best suited for robust, high-confidence characterization and identification of faulty data patterns [12]. Data conformity evaluation of tensor data was proposed for outlier identification in [13]. Without loss of generality, we describe the steps of the tensor conformity evaluation algorithm with respect to the first mode of the tensor dataset $\mathbf{D}_{(1)} \in \mathbb{R}^{(M+N+1)\times PK}$. Unfolding along the columns of the tensor we calculate the $1 \leq R_1 \leq (M+N+1)$ principal components $\mathbf{Q}_1^{(0)} \in \mathbb{R}^{(M+N+1)\times R_1}$ by solving the following maximization problem

$$\mathbf{Q}_1^{(0)} = \underset{\substack{\mathbf{Q}\in\mathbb{R}^{(M+N+1)\times R_1},\\ \mathbf{Q}^T\mathbf{Q}=\mathbf{I}_{R_1}}}{\operatorname{argmax}} \left\|\mathbf{D}_{(1)}^T\mathbf{Q}\right\|_1. \tag{8}$$

The resulting basis describes the subspace spanned by the columns of the original tensor $\mathcal{D}$ that contain nominal data. Columns that are contaminated with anomalous data are not spanned by the resulting basis vectors. We calculate the conformity of our data by computing the orthogonal projection of each column $\left[\mathbf{D}_{(1)}\right]_{:,i_1}, i_1 = 1, 2, \ldots, PK$ on the calculated subspace $\mathbf{Q}_1^{(0)}$ as

$$d_{1,i_1}^{(1)} = \left\|\mathbf{Q}_1^{(0)}\mathbf{Q}_1^{(0)^T}\left[\mathbf{D}_{(1)}\right]_{:,i_1}\right\|_2 \quad \forall i_1 = 1, 2, \ldots, PK. \tag{9}$$

Large $d_{1,i_1}^{(1)}$ values are expected if $\left[\mathbf{D}_{(1)}\right]_{:,i_1}$ is an anomalous data point and small $d_{1,i_1}^{(1)}$ values if $\left[\mathbf{D}_{(1)}\right]_{:,i_1}$ is a nominal data point. After the calculation of the projection of each column on the subspace, the conformity values are passed to a tensor $\mathcal{W}_1^{(1)} \in \mathbb{R}^{(M+N+1)\times P\times K}$

$$\mathcal{W}_1^{(1)} = \text{tensorization}\left(\left[d_{1,1}^{(1)}, \ldots, d_{1,PK}^{(1)}\right]^T \circ \mathbf{1}_{(M+N+1)\times PK}\right) \tag{10}$$

where $\mathbf{1}_{(M+N+1)\times PK}$ stands for an all-ones matrix of dimension $(M+N+1)\times LN$, and the *tensorization*$(\cdot)$ operator converts the first mode of the tensor to the original three mode tensor form. The tensor $\mathcal{W}_1^{(1)}$ contains the conformity values corresponding to each column of the original tensor $\mathcal{D}$. We repeat the above process for the rest of the modes of the original data tensor, and calculate the conformity tensors $\mathcal{W}_2^{(1)}$ and $\mathcal{W}_3^{(1)}$. We calculate the final conformity tensor $\widetilde{\mathcal{W}}^{(1)}$ by combining the above calculated tensors in an additive fashion as well as normalizing the tensor so that each element is in the $[0, 1]$ range

$$\widetilde{\mathcal{W}}^{(1)} = \frac{\sum_{k=1}^3 \alpha_k \mathcal{W}_k^{(1)} - \min\left(\sum_{k=1}^3 \alpha_k \mathcal{W}_k^{(1)}\right)}{\max\left(\sum_{k=1}^3 \alpha_k \mathcal{W}_k^{(1)}\right) - \min\left(\sum_{k=1}^3 \alpha_k \mathcal{W}_k^{(1)}\right)} \tag{11}$$

where $\alpha_1, \alpha_2, \alpha_3 \in \mathbb{R}^+, \sum_{k=1}^3 \alpha_k = 1$ correspond to weights for each mode of the tensor that model the weighting of the corresponding dimension of the original tensor. The final conformity tensor $\widetilde{\mathcal{W}}^{(1)}$ enables element-wise conformity of the original tensor data. The data conformity values can be iteratively refined until numerical convergence of the data conformity tensor $\widetilde{\mathcal{W}}^{(l)}$ for each mode of the original tensor. In Table 1, we present the pseudo-code of the proposed tensor conformity evaluation algorithm for a three mode tensor $\mathcal{X}^{I_1\times I_2\times I_3}$.

TABLE I Iterative L_1-norm tensor decomposition

Input: $\mathcal{X} \in \mathbb{R}^{I_1\times I_2\times I_3}$, ranks $R_1, R_2, R_3 \in \mathbb{Z}^+$, and weights $\alpha_1, \alpha_2, \alpha_3, \in \mathbb{R}^+, \sum_{k=1}^3 \alpha_k = 1$
Output: $\widetilde{\mathcal{W}} \in \mathbb{R}^{I_1\times I_2\times I_3}$

for k = 1, 2, 3 **do**
  $\mathbf{Q}_k^{(0)} = \underset{\substack{\mathbf{Q}\in\mathbb{R}^{I_k\times R_k},\\ \mathbf{Q}^T\mathbf{Q}=\mathbf{I}_{R_k}}}{\operatorname{argmax}} \left\|\mathbf{Q}^T\mathbf{X}_{(k)}\right\|_1$
  $M_k = \prod_{i=1, i\neq k}^3 I_i, \quad l = 1$
end for
while convergence criterion is not met **do**
  for $k = 1, 2, 3$ **do**
    $d_{k,i_k}^{(l)} = \left\|\mathbf{Q}_k^{(l-1)}\mathbf{Q}_k^{(l-1)^T}\left[\mathbf{X}_{(k)}\right]_{:,i_k}\right\|_2, \quad \forall i_k = 1, 2, \ldots, M_k$
    $\mathbf{D} = \left[d_{k,1}^{(l)} \quad \ldots \quad d_{k,M_k}^{(l)}\right]^T_{M_k\times 1} \circ \mathbf{1}_{M_k\times I_k}$
    $\mathcal{W}_k^{(l)} \leftarrow \text{tensorization}_k(\mathbf{D})$
  end for
  $\widetilde{\mathcal{W}}^{(l)} = \frac{\sum_{k=1}^K \alpha_k \mathcal{W}_k^{(l)} - \min\left(\sum_{k=1}^K \alpha_k \mathcal{W}_k^{(l)}\right)}{\max\left(\sum_{k=1}^K \alpha_k \mathcal{W}_k^{(l)}\right) - \min\left(\sum_{k=1}^K \alpha_k \mathcal{W}_k^{(l)}\right)}$
  for $k = 1, 2, 3$ **do**
    $\mathbf{Q}_k^{(l)} = \underset{\substack{\mathbf{Q}\in\mathbb{R}^{I_k\times R_k},\\ \mathbf{Q}^T\mathbf{Q}=\mathbf{I}_{R_k}}}{\operatorname{argmax}} \left\|\mathbf{Q}^T\left(\mathbf{X}_{(k)} \circ \widetilde{\mathbf{W}}_{(k)}^{(l)}\right)\right\|_1$
  end for, $l = l + 1$
end while

IV. Performance Evaluation

We test tensor data conformity evaluation for underwater object detection using RSS and AoA measurements from the deployment of an active UICSA with seven hydrophone elements and three acoustic (audio) transmitters in a 9 m deep acoustic water test tank at Florida Atlantic University. Fig. 4 depicts the locations of the UICSA and audio sources.

A. UICSA prototype

The UICSA design is based on the principles of algorithmic and mechanical compression (as depicted in Fig. 1). Compressive sensing techniques enable MUSIC-type direciton of arrival estimation of multiple acoustic sources with a sparse

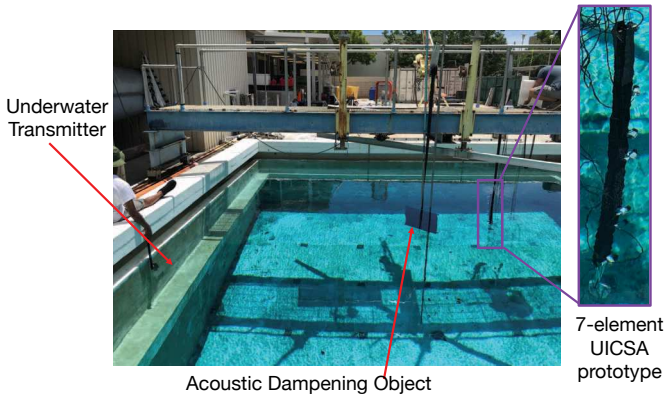

Fig. 3: Testbed deployment of UICSA and acoustic audio speakers in a 9 m deep acoustic water tank at FAU Engineering West, Boca Raton, FL.

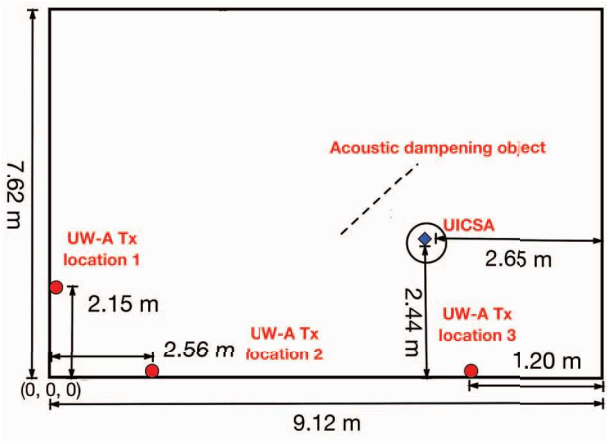

Fig. 4: Top-view schematic of the water tank setup including the location of the UICSA (blue color) and three different location for an underwater acoustic source (red color).

co-prime array. Mechanical compression enables the design of an inflatable array structure that can maintain compact size prior to deployment. Mechanical design considerations of the UICSA were first reported in [14], while preliminary experimental evaluation of the concept was conducted in [15]. We use seven Aquarian Audio $\mathrm{H2a-XLR}$ hydrophones to build the acoustic array. Each hydrophone is capable of picking up sounds from below 20 Hz to above 100 kHz. Fig. 2 shows the inter-element spacing and UICSA dimensions. We build the UICSA prototype targeting acoustic signal transmissions with a center frequency of 5 kHz ($\lambda = 0.16$ m). The length of the cables for the top four hydrophones of the array is 3 m. The bottom three hydrophone elements use 9 m cables. We use two Zoom H6 audio recorders for logging hydrophone data at the UICSA, while a GLE2016 wireless waterproof bluetooth speaker is used as an underwater acoustic source.

The UICSA includes a fairing for stowed array storage and transportation, an inflatable tubular structure, embedded sensors and holders with dedicated separation spacing to form the co-prime configuration, a buoy and an anchor to provide the force to keep the array taut once deployed. It uses an underwater pump to inject the water into the inflatable structure and let the array morph into its final geometry and maintain its stiffness. The UICSA compact package is deployed into the water tank, and the anchor can pull down the inflatable tubular structure out of the fairing. After the inflatable structure is taut, the underwater pump starts to inject water and lead the UICSA to morph into a predetermined geometry. Fig. 3 shows a close-up image of the UICSA prototype with seven hydrophone elements. After the UICSA fully inflates we examine the rich information of multi-modal tensor data recorded over time.

B. Experimental setup and results

The first hydrophone element of the array is 23 cm below the water surface (as depicted in Fig. 2). The wireless audio speaker is 35 cm below the water surface. We collect acoustic RSS and AoA measurements from three different locations in the tank. Fig. 4 depicts the locations of the UICSA The acoustic dampening object (0.9×0.5 m) is deployed 30 cm below the water surface. We consider acoustic transmission of chirp signals with duration $T = 5$ s and spanning frequencies from $f_{\min} = 2500$ Hz to $f_{\max} = 3000$ Hz.

We capture RSS and AoA data from acoustic signal transmissions from three different locations in the water tank as depicted in Fig. 4. to capture the various underwater acoustic reflections generated by underwater objects. RSS and AoA data are complementary to each other for different objects. Experiments consider the transmission of five frames from three different locations with and without an acoustic dampening object in the water tank. Fig. 5 shows RSS and AoA measurements calculated over six transmitted frames from location no. 2 in the water tank. The first four frames do not include an object in the water. A small increase in the received signal strength in the fist and second hydrophone of the UICSA in the last two frames offer an indication that the underwater environment has changed. Fig. 6a depicts algorithmically produced conformity values of the RSS and AoA measurements at the UICSA, considering acoustic transmissions from location no. 2 in the water tank. We observe that RSS conformity values for the bottom three hydrophone elements are closer to one for the first four frames, thus non-conforming with respect to the data set. Fig. 6b shows the conformity values of the RSS and AoA measurements at the UICSA, considering acoustic transmissions from all three locations in the water tank. We observe that conformity evaluation of acoustic measurements that are organized in a three-way tensor, where the third dimension corresponds to different transmitter locations, can significantly contribute toward accurate detection of underwater objects. More specifically, RSS and AoA measurements are highly non-conforming (rise toward one) for the last two frames of the data set. Consequently, it is clear that the environment has changed, once the object has been dropped underwater in the tank.

V. Conclusions

The goal of this work is to implement and evaluate a new approach for underwater target detection by leveraging a novel method to integrate multiple hydrophone sensors to a compact underwater inflatable structure. In particular, we build and experimentally evaluate a rapidly deployable active underwater inflatable co-prime sonar array. We use the array to collect RSS and AoA data from acoustic signal reflections by an underwater target. Measurements are collected for different positions of an acoustic source with respect to the array. Data

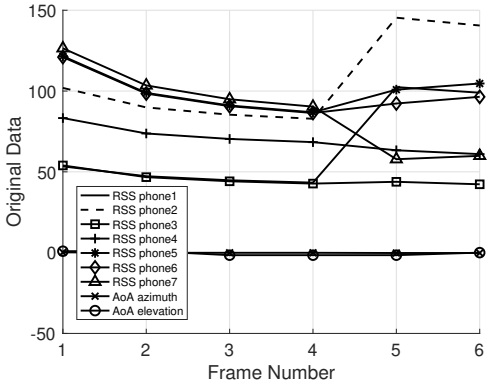

Fig. 5: Original RSS and AoA data measurements captured during acoustic transmissions from location no. 2.

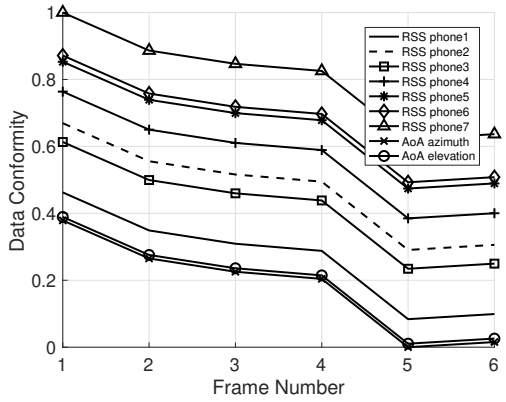

(a) Conformity values considering acoustic transmissions from location no. 2.

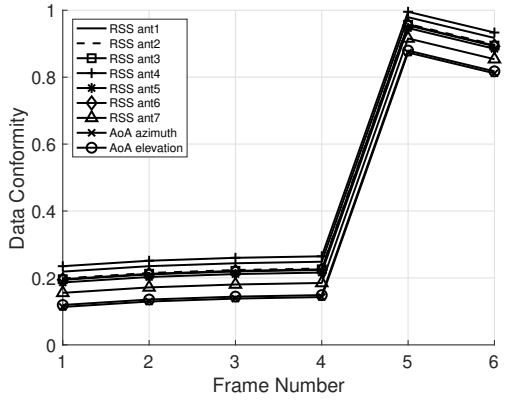

(b) Conformity values considering acoustic transmissions from all three locations.

Fig. 6: One-way vs. three-way tensor conformity evaluation for underwater target detection.

is organized in a three mode tensor. We then evaluate the conformity of each entry in the tensor with respect to all other points in the data set based on recursively refined calculations of L_1-norm tensor subspaces. Highly non-conforming data with values closer to one indicate the presence of a target in the underwater environment. We evaluate the proposed underwater target detection algorithm using RSS and AoA recordings from a co-prime array with seven hydrophone elements that is deployed in a 9 m deep acoustic water tank at Florida Atlantic University. Joint analysis of RSS and AoA data from all three source locations show significantly better target detection performance than from analyzing data from only one location.

REFERENCES

[1] E. Demirors, G. Sklivanitis, T. Melodia, S. N. Batalama, and D. A. Pados, "Software-defined underwater acoustic networks: toward a high-rate real-time reconfigurable modem," *IEEE Communications Magazine*, vol. 53, no. 11, pp. 64–71, Nov. 2015.

[2] G. Sklivanitis, Y. Cao, S. N. Batalama, and W. Su, "Distributed mimo underwater systems: Receiver design and software-defined testbed implementation," in *2016 IEEE Global Communications Conference (GLOBECOM)*, Dec. 2016, pp. 1–7.

[3] G. Sklivanitis, E. Demirors, S. N. Batalama, T. Melodia, and D. A. Pados, "Receiver configuration and testbed development for underwater cognitive channelization," in *2014 48th Asilomar Conference on Signals, Systems and Computers*, Nov. 2014, pp. 1594–1598.

[4] T. Melodia, H. Kulhandjian, L. Kuo, and E. Demirors, *Advances in Underwater Acoustic Networking*. Wiley-Blackwell, 2013, ch. 23, pp. 804–852. [Online]. Available: https://onlinelibrary.wiley.com/doi/abs/10.1002/9781118511305.ch23

[5] G. Isbitiren and O. B. Akan, "Three-dimensional underwater target tracking with acoustic sensor networks," *IEEE Transactions on Vehicular Technology*, vol. 60, no. 8, pp. 3897–3906, Oct 2011.

[6] A. Tesei, S. Fioravanti, V. Grandi, P. Guerrini, and A. Maguer, "Localization of small surface vessels through acoustic data fusion of two tetrahedral arrays of hydrophones," *Proceedings of Meetings on Acoustics*, vol. 17, no. 1, p. 070050, 2012. [Online]. Available: https://asa.scitation.org/doi/abs/10.1121/1.4772778

[7] Y. D. Zhang, M. G. Amin, and B. Himed, "Sparsity-based doa estimation using co-prime arrays," in *2013 IEEE International Conference on Acoustics, Speech and Signal Processing*, May 2013, pp. 3967–3971.

[8] C. Liu, P. P. Vaidyanathan, and P. Pal, "Coprime coarray interpolation for doa estimation via nuclear norm minimization," in *2016 IEEE International Symposium on Circuits and Systems (ISCAS)*, May 2016, pp. 2639–2642.

[9] P. P. Markopoulos, G. N. Karystinos, and D. A. Pados, "Optimal algorithms for L_1-subspace signal processing," *IEEE Trans. Signal Processing*, vol. 62, no. 19, pp. 5046–5058, Oct. 2014.

[10] P. P. Markopoulos, S. Kundu, S. Chamadia, and D. A. Pados, "Efficient L_1-norm principal-component analysis via bit flipping," *IEEE Trans. Signal Processing*, vol. 65, no. 16, pp. 4252–4264, Aug. 2017.

[11] N. Tsagkarakis, P. P. Markopoulos, G. Sklivanitis, and D. A. Pados, "L1-norm principal-component analysis of complex data," *IEEE Transactions on Signal Processing*, vol. 66, no. 12, pp. 3256–3267, June 2018.

[12] Y. Liu and D. A. Pados, "Conformity evaluation of data samples by l1-norm principal-component analysis," vol. 10658, 2018. [Online]. Available: https://doi.org/10.1117/12.2311893

[13] K. Tountas, D. A. Pados, and M. J. Medley, "Conformity evaluation and L1-norm principal-component analysis of tensor data," in *Big Data: Learning, Analytics, and Applications*, F. Ahmad, Ed., vol. 10989, International Society for Optics and Photonics. SPIE, 2019, pp. 190 – 200. [Online]. Available: https://doi.org/10.1117/12.2520538

[14] Y. Li, B. Ouyang, F. Dalgleish, A. Dalgleish, T. Su, S. Baver, J. Thomas, T. Zhou, and F. Ahmad, "Mechanical design consideration of an underwater inflatable co-prime sonar array (uicsa)," in *OCEANS 2018 MTS/IEEE Charleston*, Oct 2018, pp. 1–8.

[15] B. Ouyang, Y. Li, T. Zhou, T.-C. Su, F. Dalgleish, A. Dalgleish, and F. Ahmad, "Compressing two ways: the initial study of an underwater inflatable co-prime sonar array (uicsa)," vol. 10658, 2018. [Online]. Available: https://doi.org/10.1117/12.2311575